

J. Environ. Treat. Tech. ISSN: 2309-1185

Journal web link: http://www.jett.dormaj.com



# Mechanical Properties and Swelling Behavior of Acrylamide Hydrogels using Montmorillonite and Kaolinite as Clays

Farzaneh Sabbagh<sup>1\*</sup>, Nadia Mahmoudi Khatir<sup>2</sup>, Azam Khodaeyan Karim<sup>3</sup>, Amineh Omidvar<sup>4</sup>, Zahra Nazari<sup>5</sup>, Reza Jaberi<sup>6</sup>

- 1- Bioprocess Engineering Department, Faculty of Chemical and Energy Engineering, Universiti Teknologi Malaysia, 81310 UTM, Johor, Malaysia
  - 2- Department of Biotechnology, Faculty of Biological Science, Alzahra University, Tehran, Iran
  - 3- Department of Food Science & Technology, Quchan Branch, Islamic Azad University, Quchan, Iran 4- Department of Chemistry, Payame Noor University (PNU)
  - 5- Food quality and Safety Research Group Food Science and Technology Research Institute ACECR Mashhad Branch Mashhad, Iran
    - 6- Department of Food Science & Technology, Sabzevar Branch, Islamic Azad Univesity, Sabzevar, Iran

#### Abstract

In this study in order to increase the release ability of acrylamide hydrogels, modified acrylamide-based hydrogel nano-composites were synthesized. The aim of this research was to evaluate the swelling ratio of hydrogel with the best clay, to reach the highest rate of swelling. To enhance the swelling ratio of hydrogels, the clays were applied in their structure. Amongst the applied clays in the structure of the hydrogels, montmorillonite was found to be more effective than kaolinite. Further using conventional techniques such as X-ray diffraction (XRD) and Energy Dispersive X-Ray (EDX) performed the characterization of the clays, while the hydrogels were characterized by Fourier Transform Infrared Spectroscopy (FTIR), Field Emission Scanning Electron Microscope (FESEM), and EDX. The XRD analysis of clays showed that there is a different amount of carbon, oxygen, sodium, calcium, magnesium, aluminum, silicon, potassium and iron. The amount of oxygen in montmorillonite was 42.12 however, the amount of oxygen in kaolinite was 2.01. The XRD pattern of montmorillonite including a peak relevant to the basal dividing of  $(2\theta = 7.83^{\circ})$  11.28 Å was verified. In the acrylamide/montmorillonite hydrogels, this peak was shifted to a lower point of the angle, comparing to the basal spacing of  $(2\theta = 6.40^{\circ})$  13.78 Å and  $(2\theta = 6.24^{\circ})$  14.11 Å. Such an increase in the basal spacing oblique that the monomer was inserted into the interlayer of the clay.

Keywords: Nanoparticle, NaCMC, Microstructure, Polymerization, Nanocomposite, Crosslinker

#### 1 Introduction

Recently, the structure of hydrogels has been blended by strengthening the nanostructures to polymerize a nanocomposite hydrogel in order to make changes in physical, mechanical and material properties (1). The cross-linked structures in the three-dimensional systems, provide the nanocomposite hydrogels which have similarities with the layers in clay silicate (2). Some of the useful applications of hydrogels including drug delivery devices and wound dressing systems (3,4). The major concerns on the hydrogels with clay-polymer structure are focused on montmorillonite, laponite, and hydrotalcite as some improved factors. The reasons that the clays are highly utilized for different medical applications is that they owe unique physicochemical qualities

Corresponding author: Farzaneh Sabbagh, Department of Bioprocess Engineering, Faculty of Chemical Engineering, Universiti Teknologi Malaysia, 81310. Email: farzaneh2464@yahoo.com and smfarzaneh2@live.utm.my. Telephone: 0060-177768087.

and very specific surface zone in their structure (5-8). Clay is an organically tailored phyllosilicate, which is derived from an organically occurring clay mineral. The clay minerals are very effective in the polymer structure, because they have small particle size and have intercalation properties, and are hydrated layered aluminosilicate with reactive -OH groups on their surface. The factors such as pH, temperature and other environmental conditions are able to impact on the hydrogels and the hydrogels can react to these factors as they are very powerful materials (8,9). By locating of hydrophilic groups such as amide, sulfonic acid, the hydroxyl group and carboxylic acid in their structure, the hydrogels start to absorb a large amount of water, they swell and can produce hydrophilic polymers (10-12). To improve the physical properties of hydrogels, they can be added by novel applicable arrangements (13). Due to their stability under violent conditions of procedure for health, they are very exciting by locating of metal oxides such as MgO (14-17). The MgO nanoparticles have various biomedical advantages (18). The role of clays in pharmaceutical products is excipient and active ingredients. Amongst all

the clays, montmorillonite has attracted more attention due to having more capacity of cation exchange rather than the rest of pharmaceutical silicates such as kaoline, talc, and fibrous clay minerals (19). The composition of clay/polymer composites has improved mechanical properties (20). These facts of interest along with the high limit of interaction that is proposed by mineral particles have been generally initiated to clarify novel systems of controlled release yet sometimes it is necessary to modify polymeric material or clay minerals. Polyacrylamide is a kind of pH-sensitive hydrogel (21,22).

The aim of this study is to reach to the highest swelling ratio in the hydrogels containing two different clays. We are evaluating some characterizations and also the highest swelling ratio between Montmorillonite and Kaolinite and then apply one of them in the structure of hydrogel.

# 2 Experimental Methodologies

#### 2.1 Materials

Acrylamide (Aam) and MgO applied in this research study were provided from Sigma-Aldrich Chemical Company. *N*,*N*'-methylene bisacrylamide (MBA) as the crosslinker, the activator *N*,*N*,*N*', *N*'-tetramethyl ethylenediamine (TEMED) and the initiator ammonium persulfate (APS) were completely analytical grade and were purchased from Sigma-Aldrich Chemical Company. Deionized water was applied during the experiments in the formulation of hydrogels in the swelling experiments, Kaolin powder with 98% purity and montmorillonite (MMT), with an average particle size of 1 μm was used with no further modification. All the material was obtained from Sigma-Aldrich Malaysia and supplementary chemicals and reagents applied were entirely analytical grade.

### 2.2 Formulation of Acrylamide/NaCMC/MgO Nanocomposites

Acrylamide/NaCMC/MgO nanocomposite was accumulated by mixing 0.01 g MgO nanoparticles (<50nm) and 0.01 g clay with the polymer matrix. First, MgO was weighing for 0.01 g and poured into 2 ml of distilled water at 80 °C under vigorous stirring. Acrylamide, ammonium persulfate (APS), N,N. tetramethylethylenediamine (TEMED), sodium carboxymethylecellulose (NaCMC), N. N'methylenebisacrylamide (MBA), was added to the solution, after nearly 10 minutes. The whole duration of polymerization of nano complex took about 40 mins [23].

## 2.3 XRD analysis

For the X-ray diffraction of Kaolinite and Montmorillonite, the clays were subjected to x-beam diffraction (XRD)  $K\alpha$  at 40keV and 40mA was applied with a step. length of  $0.05^{\circ}$  and step time of 1s. The used diffraction

edge ( $2\theta$ ) was in the range of 20 ° and 80 °. An x-beam diffraction amount of clay was carried out at 25 °C with Siemens. Diffractometer D5000 X-beam diffractometer along with Cu (24).

#### 2.4 FTIR Analysis

The FTIR spectrum of hydrogels was taken in the range of 4000-370 cm<sup>-1</sup> as KBr pellet with the help of FTIR (Nicolet. 670 FTIR, USA) were analyzed. Amount of 4 mg of the dried specimens of hydrogels were weighing and blended with Potassium Bromide (25).

#### 2.5 Hydrogel Nano Composites Microstructure

To consider the microstructure of hydrogels, Field emission scanning electron microscope (FESEM) (35VP Gemini Supra) was applied. This was done under vacuum condition and employing gold sputter coater Bio-Rad Polaran Division (E6700, USA). The voltage of 10 kV was carried out using the amplification of 3000× and 9000×. To keep the samples pores wholesome for preparing to image, all of them were lyophilized and were placed in liquid (26).

#### 2.6 Swelling Studies

Immersing the samples in distilled water conducted to make them ready for swelling ratio analysis. Occasionally, the weight of the swelling ratio was measured and then computed by means of the following equation:

Swelling ratio (%) = 
$$\left[\frac{Wt - W0}{W0}\right] \times 100$$
 (Equation 1)

The weight of the swollen gels is designed by Wt at time t and  $W_0$  is the beginning weight of the samples (27).

# 3 Results and Discussion

#### 3.1 Reagents

The presence of all of the elements that constitutes the montmorillonite and kaolinite clay mineral may be observed, indicating its effective incorporation (Table 1) was determined by using elemental analysis, which resulted in the unit cell formula. Apparently, the chemical compositions breakdown of clay shows the main dominant elements in the clay were (O=Oxygen), (C=Calcium), (Na= Sodium), (Mg= Magnesium), (Fe= Iron), (Si=Silicon), (K=Potassium), (Al=Aluminum). The EDX profile of montmorillonite and kaolinite (Figure 1 (a) and (b)) shows that the percentage of Si and Al in the montmorillonite and kaolinite is 9.97% and 19.90%, and 17.18% and 5.96% respectively. Whereas the percentages of other metals like K, Na, Ca, Mg, O and Fe is, 0.19%, 0, 0, 0, 2.01%, in kaolinite and 0.41%, 0.32%, 0.49%, 0.79% and 42.12% in montmorillonite. The major constituents of the clay are aluminum, silicon, magnesium, iron, oxygen and calcium, which correspond to its chemical formula.

Table 1: EDX analysis of Kaolinite and Montmorillonite

Clays/ Elements	C	0	Na	Ca	Mg	Al	Si	×	Fe
Kaolinite (weight%)	6.54	2.01	1	ı	1	17.18	19.90	0.19	1
Montmorillonite (weight%)	6.97	42.12	0.32	0.49	0.79	5.96	9.97	0.41	0.62

The representing of O and Si components, coming absolutely from the clay mineral, suggests that good element dispersion occurred in the clay matrix (Figure 1). So as to consider the composition of montmorillonite and kaolinite, XRD test was accomplished (Figure 1). The crystallinity changes of samples with clays were considered to have a better understanding of hydrogel structural stability and network.

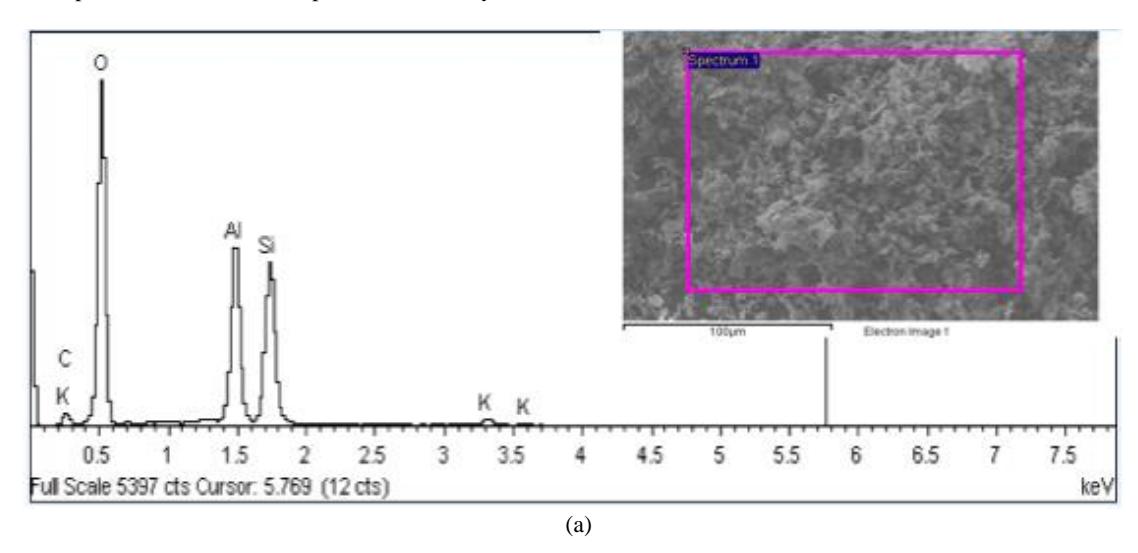
The large surface area of Kaolinite and montmorillonite and/or their extensive pharmaceutical application are the main reasons to choose them. The properties of such different clays are related to their composition and structure (Figure 2). The montmorillonite clays are 2:1 phyllosilicates stacked single sheets of tetrahedral silica on top of a single sheet of octahedral alumina however, kaolinite consists of 1:1 (28). The way that the layers are stacked on each other detects the differences in the kaolin minerals. The interlayer in montmorillonite is not only expansible, but it is also hydrated; That is the reason, they are called to as "swelling clays" (29).

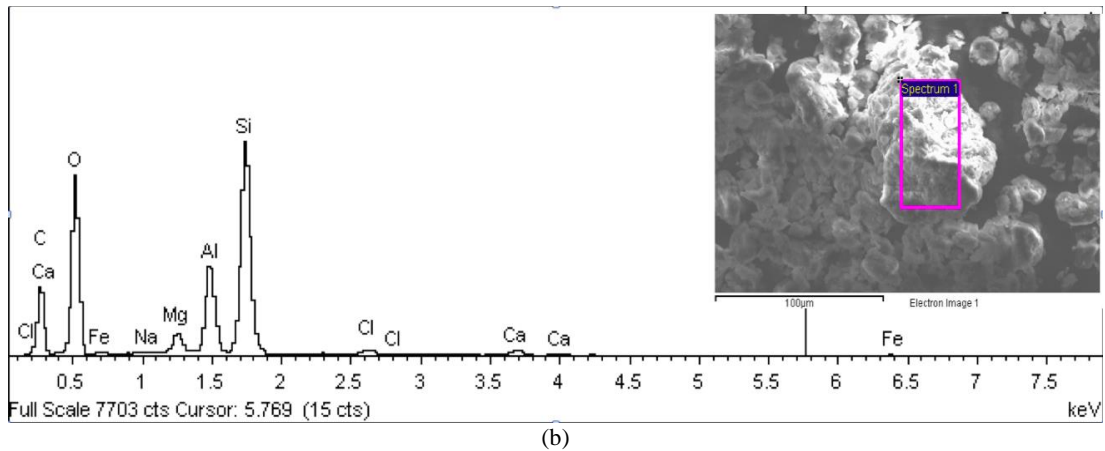
#### 3.2 XRD pattern of Clays

The X-ray diffraction performed for the clays are presented in Figure.3.X-ray diffraction was a useful tool to test the possible orientation and penetration of clays in

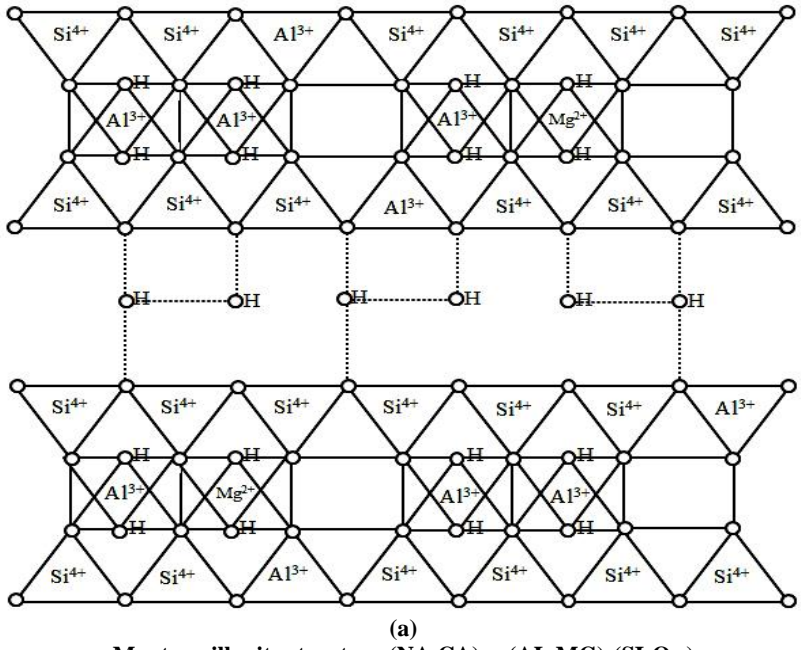
the interlayer space of smectites, by revealing changes in the basal spacing of the clay minerals (30). The XRD pattern of kaolinite is presented in figure 3(a) and the XRD pattern of montmorillonite is presented in figure 3(b).

The diffraction pattern of montmorillonite including a peak relevant to the basal dividing of  $(2\theta = 7.83^{\circ})$ 11.28 Å was verified. In the acrylamide/montmorillonite hydrogels, this peak was shifted to a lower point of the angle, comparing to the basal spacing of  $(2\theta = 6.40^{\circ})$ 13.78 Å and  $(2\theta = 6.24^{\circ})$  14.11 Å. Such an increase in the basal spacing oblique that the monomer was inserted into the interlayer of the clay. This is due to the polymerization of acrylamide monomer to polyacrylamide matrix that gave a contraction between layers of the montmorillonite (31). A flattened conformation was adopted between the layers of the clay in the polymer. It is concluded that in composite hydrogels the clay minerals were intercalated but not exfoliated and authoritatively disseminated in the matrix. Small molecules (kaolinite) were weakly bound to the clay mineral and no significant changes in the basal spacing of the complexes were observed after desorption, whereas for promethazine important modifications in the X-ray were reported (32).

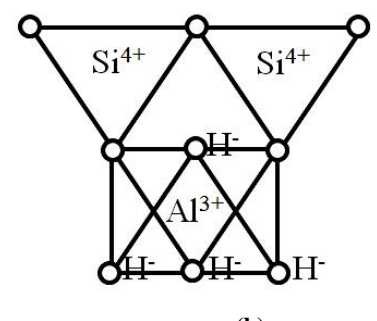




 $Figure \ 1: Energy \ Dispersive \ X-Ray \ (EDX) \ spectrum \ of \ clay \ Montmorillonite (a) \ and \ Kaolinite \ (b)$ 



 $Montmorillonite\ structure\ (NA,CA)_{0.33}(AL,MG)_2(SI_4O_{10})$ 



(b) Kaolinite structure Al<sub>2</sub>Si<sub>2</sub>O<sub>5</sub>(OH<sub>4</sub>)

Figure 2: Chemical structure of (a) Montmorillonite and (b) Kaolinite

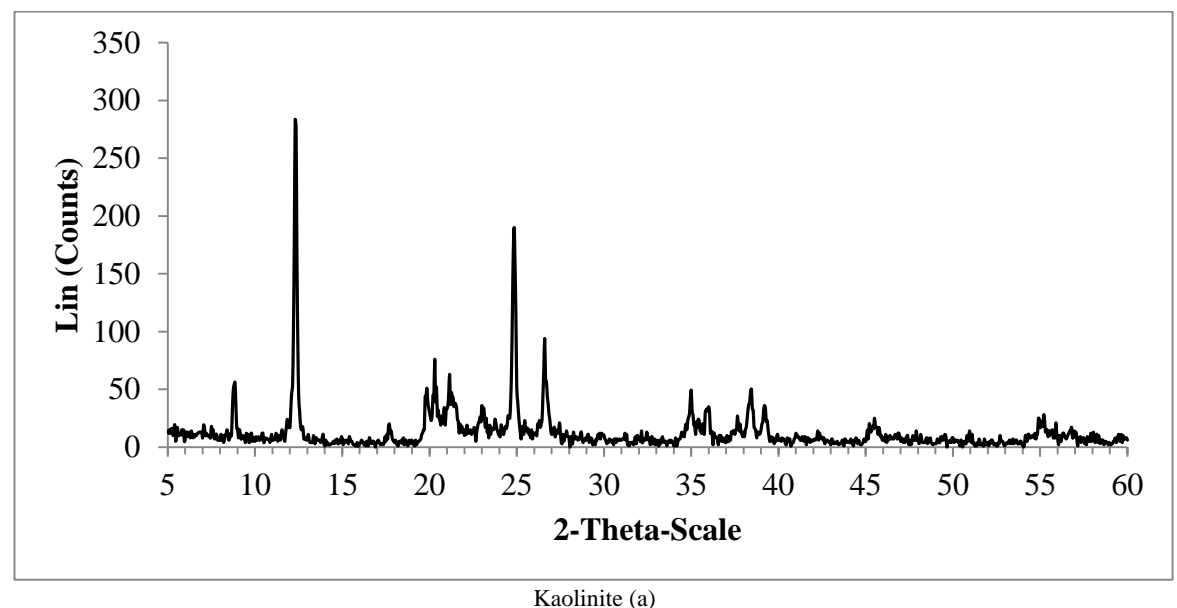
## 3.3 Polymerization

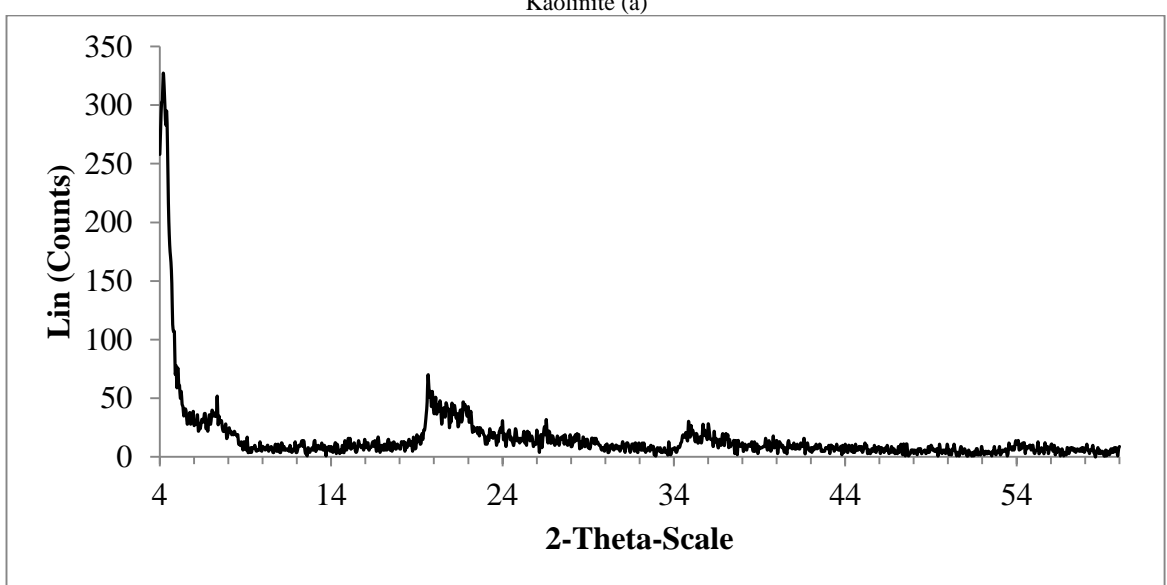
The polymerization of acrylamide hydrogels is happening in the presence of smaller amount of bisacrylamide. Bisacrylamide essentially is linked to two acrylamide molecules by a methylene group, and is applied as crosslinking agent. A second site to extend the chain is introduced due to polymerization of acrylamide monomer in the head to tail order and producing bisacrylamide molecules into long chains. The polymerization of acrylamide monomer is free radical's catalysis, and by the addition of TEMED and APS is initiated. The TEMED role in the matrix is catalyzer of the decomposition of persulphate ion and presents free radical. Hydrogel composites were shaped by some interaction and conglomeration with acrylamide in montmorillonite interlayer gallery. Acrylamide/montmorillonite composite hydrogel and Acrylamide/ kaolinite composite hydrogel were the result of free radical polymerization in distilled water containing of clay in optimized ratio of acrylamide to clay (6:1%, w/w), APS and TEMED were added as the initiator and accelerator, respectively. The content of the clay is very important. At lower contents of clay, the polymer/clay systems could have a tendency to produce disordered phases as nematic or isotropic, an increase of polymer chain length and/or organ clay content leads to the creation of ordered phases (crystal, smectic or columnar) (33).

# 3.4 Swelling ratio study

According to the outcomes, the specifications of acrylamide hydrogel were encouragingly transformed by incorporating with clays. The two mentioned clays were applied in the hydrogels and were placed in distilled water to determine the swelling ratio (Figure 4). By comparing these samples, Montmorillonite had the greatest swelling ratio rather than kaolinite.

In Figure 4, the swelling ratio of the hydrogel in distilled water is presented and by NaCMC addition, the quantity of swelling was found to be increased to a greater level. On the other hand, the presence of multitude carboxylic acid groups in its structure is very effective. The presence of hydrophilic chains on the polymeric chains (–COOCH<sub>3</sub>Na) and (–OH) and hydration of functional groups was responsible for the swelling of the hydrogels.





Montmorillonite (b)
Figure 3: XRD pattern of Kaolinite (a) and Montmorillonite (b)

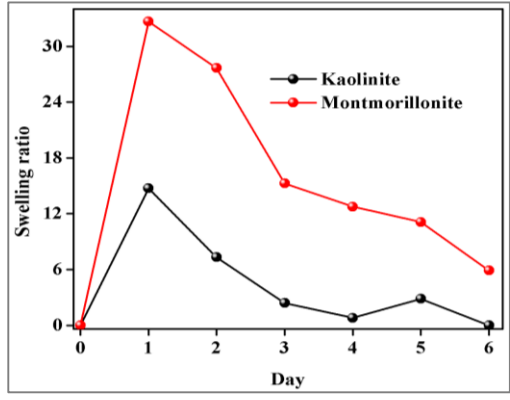


Figure 4: Swelling ratio of Kaolinite and Montmorillonite clays using in the acrylamide-based hydrogels

According to our previous reports (34), by expanding the swelling ability of hydrogels, the drug release and loading components within the hydrogel network are enhanced owing to the aggregate permeability of hydrogels that give them the ability to release the trapped drugs easier. However, it is seen that acrylamide hydrogels in establishment with montmorillonite swells faster than the hydrogels incorporation with kaolinite. This fact could be explained by the presence of strongly hydrophilic clay that attracts water at the beginning of swelling much faster than the kaolinite with different structure rather than montmorillonite (35).

## 3.5 Characterization of Modified Acrylamide Based-Hydrogel Nanocomposites

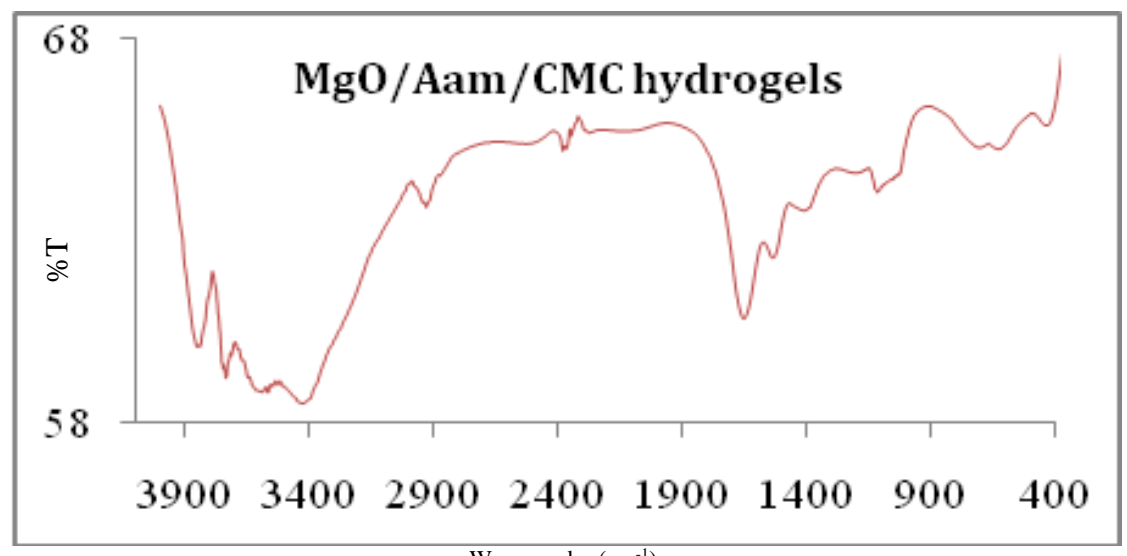
# 3.5.1 FTIR Characterization

The Figure 5 represents the synthesis of acrylamidebased hydrogels obtained from the FTIR spectra. The peak for ester groups was found around 703. The peak of 2368 relates to silicon capacity and the peak of 1650 cm<sup>-1</sup> is a result of amide-I of acrylamide units (36). The peak 2929 cm<sup>-1</sup> is for presence of C–N and C–H extending groups, separately, further affirming the trend of the amide group. The extending of –OH gatherings result in peak 3421 cm<sup>-1</sup>. The peak at 1023 cm<sup>-1</sup> advocated –CH–O–CH– extending. The peak is seen at 1650 cm<sup>-1</sup> was a direct result of the amide-I band of the amide group of polyacrylamide (>C = O stretching vibration frequency). The amide-I band was relocated from 1661cm<sup>-1</sup>, in the cross-connected polyacrylamide, to 1650cm<sup>-1</sup>. The peaks at 1023 cm<sup>-1</sup> in the FTIR range is normal for skeletal vibration including the extending of C–O bonds in anhydrous glucose units. The peaks at 2929 cm<sup>-1</sup> indicated C–H stretching of – CH<sub>2</sub> groups. This infers that due to the less steric restriction of the hydroxyl group, the hydroxyl group of acrylamide is the favored site for the response with the crosslinker and the joining of acrylamide (37).

#### 3.5.2 FESEM, EDX analysis

The dynamic swelling behavior of hydrogels depends on the relative contribution of penetrant diffusion and relaxation of crosslinked polymer chains. It was until affirmation the outcome of nanoparticles on the microstructure of hydrogel, FESEM/EDX of the clear hydrogel and the nanoparticles-stacked hydrogels were considered as demonstrated in Figure 6. Field Emission Scanning Electron Microscopy (FESEM) analysis was carried out

with minor modification. FESEM was performed in order to assess the surface characterization of hydrogels (38). Polyacrylamide containing Kaolin and montmorillonite microparticles have macro porous structure with average diameter of pore size less than 1 µm. MgO nanoparticles organized the initial burst release organized through modification of polymeric complex and by affecting the release mechanism (39,40). The FESEM images magnifications were undergone at 2.0K×. Apparently, stacking nanoparticles had changed the surface morphology of the clear hydrogel. This shows the arrangement of nanoparticles in the system of the clear hydrogel, while the clear hydrogel uncovered clear systems through the gel association. Also, it is clear that nanofillers produce a same type of structure once integrated into the blank matrix, which was more evident in the magnetic type of nanocomposites. Making of nanoparticles inside the hydrogel system brings about moving the porosity of hydrogels. It can be seen that the nanoparticles have effectively unbroken apportion through the hydrogel organizes as demonstrated in Figure.7. The EDX range moreover supports the arrangement of metal nanoparticles in the hydrogels (41).



Wavenumber(cm<sup>-1</sup>)
Figure 5: FTIR spectra for acrylamide-based hydrogels

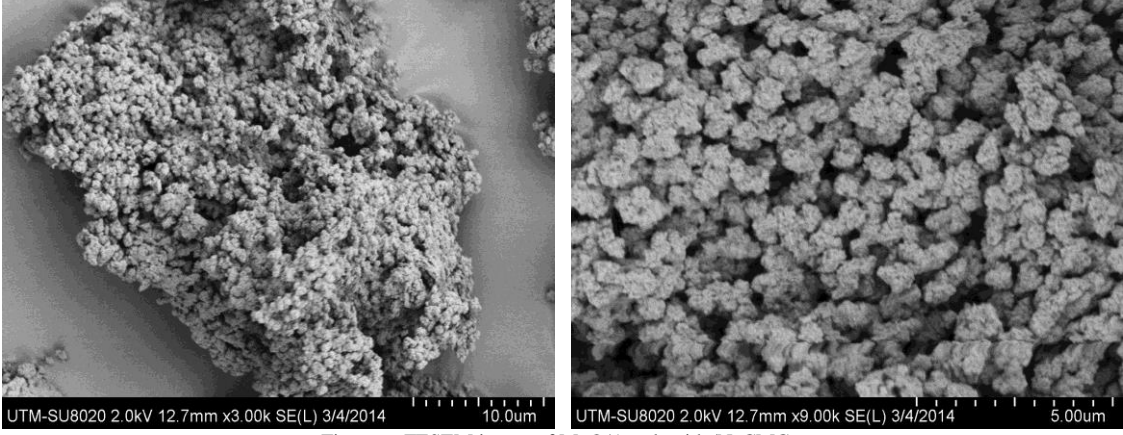


Figure 6: FESEM image of MgO/Acrylamide/NaCMC

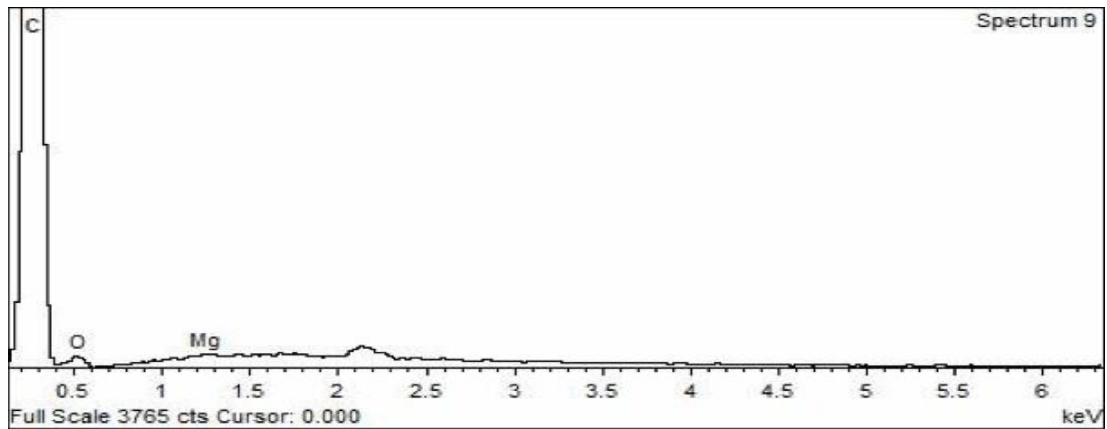


Figure 7: EDX of MgO/Acrylamide/NaCMC hydrogels

# **4 Conclusion**

The layered silicate materials such as montmorillonite, have drawn a great deal of attention because of its ability to release drugs in a controlled mode, ultimately leading to high value of drug. Polyacrylapolyacrylamide/kaolinite mide/montmorillonite and composites were obtained by polymerization. Network parameters and Swelling behavior of hydrogels were studied. The study results indicated that the montmorillonite is the best clay to be applied in the hydrogel among the clays, due to its highest swelling ratio. Addition of nanoparticles changed the water-uptake in hydrogels by direct water adsorption (at the water interface), and changing the network density (by adding physical crosslink points to the existing chemical crosslinks). By adding the MgO to the monomer system the greater swelling capacity of the MgO hydrogels can be attributed to the presence of MgO nanoparticles with different surface charges, size, and morphology. The MgO nanoparticles caused in the dispersion of more water molecules to equilibrate the buildup ion osmotic pressure, which resulted in swelling. As a future recommendation, it can be suggested to apply two clays with the highest abilities in the swelling and thus to reach to highest amount of release in the drug delivery systems.

### **Conflicts of interest**

The authors have no conflicts of interest.

# **Ethical issue**

Authors are aware of, and have complied with the best practice in publication ethics specifically with regard to authorship, dual submission, and manipulation of figures, competing interests and compliance with policies on research ethics. Authors have adhered to publication requirements that this submitted work is original and has not been published elsewhere in any form of language.

## **Competing interests**

The authors wish to declare that there is no conflict of interest in this research work.

## **Authors' contribution**

All the authors of this study have completely contributed to the data collection, data analyses and manuscript writing.

#### References

- [1] Gholizadeh, H., Cheng, S., Pozzoli, M., Messerotti, E., Traini, D., Young, P., Kourmatzis, A., Ong, HX. Smart thermosensitive chitosan hydrogel for nasal delivery of ibuprofen to treat neurological disorders. Expert opinion on drug delivery, 2019.
- [2] Ruskowitz, ER., Comerford, MP., Badeau, BA., DeForest, CA. Logical stimuli-triggered delivery of small molecules from hydrogel biomaterials. Biomaterials science, 2019.7(2): p.542-546.
- [3] Jämstorp Berg, E. Diffusion controlled drug release from slurry formed, porous, organic and clay-derived pellets (Doctoral dissertation, Acta Universitatis Upsaliensis).
- [4] Nesrinne, S., Djamel, A. Synthesis, characterization and rheological behavior of pH sensitive poly (acrylamide-co-acrylic acid) hydrogels. Arabian Journal of Chemistry, 2017. 10(4): p. 539-547.
- [5] Duncan, J., MacDonald, JF., Hanna, JV., Shirosaki, Y., Hayakawa, S., Osaka, A., Skakle, JM., Gibson, IR. The role of the chemical composition of monetite on the synthesis and properties of α-tricalcium phosphate. Materials Science and Engineering: C, 2014.1(34): p.123-129.
- [6] Dragan, ES., Lazar, MM., Dinu, MV., Doroftei, F. Macroporous composite IPN hydrogels based on poly (acrylamide) and chitosan with tuned swelling and sorption of cationic dyes. Chemical engineering journal, 2012. 15(204): p. 198-209.
- [7] Dinu, MV., Perju, MM., Drăgan, ES. Composite IPN ionic hydrogels based on polyacrylamide and dextran sulfate. Reactive and Functional Polymers, 2011. 71(8): p. 881-890.
- [8] Guiseppi-Elie, A., Koch, L., Finley, SH., Wnek, GE. The effect of temperature on the impedimetric response of bioreceptor hosting hydrogels. Biosensors and Bioelectronics, 2011. 26(5): p. 2275-2280.
- [9] Kevadiya, BD., Pawar, RR., Rajkumar, S., Jog, R., Baravalia, YK., Jivrajani, H., Chotai, N., Sheth, NR., Bajaj, HC. pH responsive MMT/acrylamide super composite hydrogel: characterization, anticancer drug reservoir and controlled release property. Biochem Biophys, 2013. 1(3):p. 43-60.
- [10] Leal, D., De Borggraeve, W., Encinas, MV., Matsuhiro, B., Müller, R. Preparation and characterization of hydrogels based on homopolymeric fractions of sodium alginate and PNIPAAm. Carbohydrate polymers, 2013. 92(1):p.157-166.
- [11] Mittal, H., Jindal, R., Kaith, BS., Maity, A., Ray, SS. Flocculation and adsorption properties of biode-

- gradable gum-ghatti-grafted poly (acrylamide-comethacrylic acid) hydrogels. Carbohydrate polymers, 2015. 22(115): p.617-628.
- [12] Singh, B., Sharma, V. Influence of polymer network parameters of tragacanth gum-based pH responsive hydrogels on drug delivery. Carbohydrate polymers, 2014. 30(101): p.928-940.
- [13] Huh, HW., Zhao, L., Kim, SY. Biomineralized biomimetic organic/inorganic hybrid hydrogels based on hyaluronic acid and poloxamer. Carbohydrate polymers, 2015. 1(126): p.130-140.
- [14] Samanta, HS., Ray, SK. Synthesis, characterization, swelling and drug release behavior of semiinterpenetrating network hydrogels of sodium alginate and polyacrylamide. Carbohydrate polymers, 2014. 2(99): p. 666-678.
- [15] Zhu, Y., Jiang, H., Ye, SH., Yoshizumi, T., Wagner, WR. Tailoring the degradation rates of thermally responsive hydrogels designed for soft tissue injection by varying the autocatalytic potential. Biomaterials, 2015. 1(53): p.484-493.
- [16] Dragan, ES., Perju, MM., Dinu, MV. Preparation and characterization of IPN composite hydrogels based on polyacrylamide and chitosan and their interaction with ionic dyes. Carbohydrate polymers, 2012. 88(1): p.270-281.
- [17] Muhamad, II., Sabbagh, F., A Karim, NA. Polyhy-droxyalkanoates: a valuable secondary metabolite produced in microorganisms and plants. Plant Secondary Metabolites, Volume Three: Their Roles in Stress Eco-Physiology, 2017. 6: p. 185.
- [18] Ohira, T., Yamamoto, O. Correlation between antibacterial activity and crystallite size on ceramics. Chemical engineering science, 2012. 68(1): p. 355-361
- [19] Kenne, L., Gohil, S., Nilsson, EM., Karlsson, A., Ericsson, D., Kenne, AH., Nord, LI. Modification and cross-linking parameters in hyaluronic acid hydrogels—definitions and analytical methods. Carbohydrate polymers, 2013. 91(1): p. 410-418.
- [20] Dash, R., Foston, M., Ragauskas, AJ. Improving the mechanical and thermal properties of gelatin hydrogels cross-linked by cellulose nanowhiskers. Carbohydrate polymers, 2013. 91(2): p.638-645.
- [21] Rani, M., Agarwal, A., Maharana, T., Negi, YS. A comparative study for interpenetrating polymeric network (IPN) of chitosan-amino acid beads for controlled drug release. African Journal of Pharmacy and Pharmacology, 2010. 4(2): p.035-054.
- [22] Shalviri, A., Liu, Q., Abdekhodaie, MJ., Wu, XY. Novel modified starch–xanthan gum hydrogels for controlled drug delivery: Synthesis and characterization. Carbohydrate Polymers, 2010. 79(4): p.898-907.
- [23] Sabbagh, F., Muhamad, II. Acrylamide-based hydrogel drug delivery systems: release of acyclovir from MgO nanocomposite hydrogel. Journal of the Taiwan Institute of Chemical Engineers, 2017. 1(72):p.182-193.
- [24] Santhanam, A., Sasidharan, S. Microbial production of polyhydroxy alkanotes (PHA) from Alcaligens spp. and Pseudomonas oleovorans using different carbon sources. African Journal of Biotechnology, 2010.9(21):p.3144-3150.
- [25] Sabbagh, F., Muhamad, II. Physical and chemical characterisation of acrylamide-based hydrogels, Aam, Aam/NaCMC and Aam/NaCMC/MgO. Journal

- of Inorganic and Organometallic Polymers and Materials, 2017. 27(5):p.1439-1449.
- [26] Yang, X., Guo, L., Fan, Y., Zhang, X. Preparation and characterization of macromolecule cross-linked collagen hydrogels for chondrocyte delivery. International journal of biological macromolecules, 2013. 1(61): p.487-493.
- [27] Akalp, U., Chu, S., Skaalure, SC., Bryant, SJ., Doostan, A., Vernerey, FJ. Determination of the polymer-solvent interaction parameter for PEG hydrogels in water: Application of a self learning algorithm. Polymer, 2015. 1(66):p.135-147.
- [28] Sabbagh, F., Muhamad, II., Nazari, Z., Mobini, P., Khatir, NM. Investigation of acyclovir-loaded, acrylamide-based hydrogels for potential use as vaginal ring. Materials Today Communications, 2018. 1(16): p.274-280.
- [29] Sirousazar, M., Kokabi, M., Hassan, ZM. In vivo and cytotoxic assays of a poly (vinyl alcohol)/clay nanocomposite hydrogel wound dressing. Journal of Biomaterials Science, Polymer Edition. 2011. 22(8):p.1023-1033.
- [30] Bostan, MS., Senol, M., Cig, T., Peker, I., Goren, AC., Ozturk, T., Eroglu, MS. Controlled release of 5aminosalicylicacid from chitosan based pH and temperature sensitive hydrogels. International journal of biological macromolecules, 2013. 1(52):p. 177-183.
- [31] Sabbagh, F., Muhamad, II., Nazari, Z., Mobini, P., Taraghdari, SB. From formulation of acrylamidebased hydrogels to their optimization for drug release using response surface methodology. Materials Science and Engineering: C, 2018. 1(92): p. 20-25.
- [32] Jensen, AT., Neto, WS., Ferreira, GR., Glenn, AF., Gambetta, R., Gonçalves, SB., Valadares, LF., Machado, F. Synthesis of polymer/inorganic hybrids through heterophase polymerizations. InRecent Developments in Polymer Macro, Micro and Nano Blends, 2017. 1 (p. 207-235). Woodhead Publishing.
- [33] van Keulen, H., Asseng, S. Simulation models as tools for crop management. Encyclopedia of Sustainability Science and Technology. 2018. p.1-20.
- [34] García, MC., Uberman, PM. Nanohybrid Filler-Based Drug-Delivery System. InNanocarriers for Drug Delivery, 2019. 1 (p. 43-79). Elsevier.
- [35] Popa, L., Ghica, MV., Dinu-Pîrvu, CE. Hydrogels-Smart Materials for Biomedical Applications.
- [36] Aguilar, MR., San, Román J. Introduction to smart polymers and their applications. In Smart polymers and their applications, 2019. 1 (p. 1-11). Woodhead Publishing.
- [37] Sabbagh, F., Muhamad, II. Production of polyhydroxyalkanoate as secondary metabolite with main focus on sustainable energy. Renewable and Sustainable Energy Reviews, 2017. 1(72):p.95-104.
- [38] Batista, AH., Rate, AW., Gilkes, RJ., Saunders, M., Dodd, A. Scanning and transmission analytical electron microscopy (STEM-EDX) can identify structural forms of lead by mapping of clay crystals, Geoderma 2018 15(310):p.191-200.
- [39] Sankaran, S., Becker, J., Wittmann, C., del Campo, A. Optoregulated drug release from an engineered living hydrogel.
- [40] Puspitasari, T., Raja, KM., Pangerteni, DS., Patriati, A., Putra, EG. Structural organization of poly (vinyl alcohol) hydrogels obtained by freezing/thawing and γ-irradiation processes: A small-angle neutron

- scattering (SANS) study. Procedia Chemistry, 2012. 1(4):p.186-193.
- [41] Montero, A., Valencia, L., Corrales, R., Jorcano, J. L., & Velasco, D. (2019). Smart Polymer Gels: Propdhead Publishing.

erties, Synthesis, and Applications. In Smart Polymers and their Applications (p. 279-321). Woo